

Normal energy and stretch diffusion in a one-dimensional momentum conserving lattice with nonlinear bounded kinetic energy

Hongbin Chen(陈宏斌), Qin-Yi Zhang(张钦奕), Jiahui Wang(王佳惠), Nianbei Li(李念北), and Jie Chen(陈杰)
Citation: Chin. Phys. B, 2025, 34 (**9**): 094401. DOI: 10.1088/1674-1056/addce5
http://cpb.iphy.ac.cn; http://iopscience.iop.org/cpb

What follows is a list of articles you may be interested in

Theoretical study on the effective thermal conductivity of silica aerogels based on a cross-aligned and cubic pore model

Kuncan Zheng(郑坤灿), Zhendong Li(李震东), Yutong Cao(曹豫通), Ben Liu(刘犇)), and Junlei Hu(胡君磊)
Chin. Phys. B, 2024, 33 (**6**): 064401. DOI: 10.1088/1674-1056/ad47ac

Thermal transport in composition graded silicene/germanene heterostructures

Zengqiang Cao(曹增强), Chaoyu Wang(王超宇), Honggang Zhang(张宏岗), Bo You(游波), and Yuxiang Ni(倪宇翔)
Chin. Phys. B, 2024, 33 (**4**): 044402. DOI: 10.1088/1674-1056/ad1500

Lattice Boltzmann simulation on thermal performance of composite phase change material based on Voronoi models

Meng-Yue Guo(郭孟月), Qun Han(韩群), Xiang-Dong Liu(刘向东), and Bo Zhou(周博)
Chin. Phys. B, 2021, 30 (**10**): 104401. DOI: 10.1088/1674-1056/ac041d

Establishment and evaluation of a co-effect structure with thermal concentration-rotation function in transient regime

Yi-yi Li(李依依), Hao-chun Zhang(张昊春)
Chin. Phys. B, 2020, 29 (**8**): 084401. DOI: 10.1088/1674-1056/ab9437

Uniformity principle of temperature difference field in heat transfer optimization

Xue-Tao Cheng(程雪涛), Xin-Gang Liang(梁新刚)
Chin. Phys. B, 2019, 28 (**6**): 064402. DOI: 10.1088/1674-1056/28/6/064402

SPECIAL TOPIC — Heat conduction and its related interdisciplinary areas

Normal energy and stretch diffusion in a one-dimensional momentum conserving lattice with nonlinear bounded kinetic energy

Hongbin Chen(陈宏斌)[1], Qin-Yi Zhang(张钦奕)[1], Jiahui Wang(王佳惠)[1], Nianbei Li(李念北)[1,†], and Jie Chen(陈杰)[2,‡]

[1] *Institute of Systems Science and Department of Physics, College of Information Science and Engineering, Huaqiao University, Xiamen* 361021, *China*

[2] *Center for Phononics and Thermal Energy Science, China–EU Joint Laboratory for Nanophononics, MOE Key Laboratory of Advanced Micro-structured Materials, School of Physics Science and Engineering, Tongji University, Shanghai* 200092, *China*

(Received 7 April 2025; revised manuscript received 16 May 2025; accepted manuscript online 27 May 2025)

One-dimensional (1D) nonlinear lattices that conserve momentum exhibit anomalous heat conduction, except for the specific case of the 1D coupled rotator lattice. Unlike classical interacting 1D nonlinear lattices such as the Fermi–Pasta–Ulam β (FPU-β) lattice, the 1D coupled rotator lattice has a bounded interaction potential energy. Recently, the 1D coupled rotator lattice with additional bounded kinetic energy has also been found to exhibit normal heat conduction. Here, we study energy diffusion in the 1D momentum-conserving lattice with bounded kinetic energy only. We find that this lattice exhibits normal energy diffusion as well as normal stretch diffusion. This work indicates that bounded energy, whether kinetic or potential, is crucial for normal energy diffusion and heat conduction in 1D momentum-conserving nonlinear lattices.

Keywords: heat conduction, nonlinear dynamics

PACS: 44.10.+i, 05.45.–a

DOI: 10.1088/1674-1056/addce5 **CSTR:** 32038.14.CPB.addce5

1. Introduction

One-dimensional (1D) nonlinear lattices with interaction potential energy, such as the Fermi–Pasta–Ulam β (FPU-β) lattice, exhibit anomalous heat conduction,[1] where their heat conductivities κ diverge with the lattice length L in a power-law fashion as $\kappa \propto L^{\alpha}$ with $0 < \alpha < 1$.[2–14] In contrast, 1D nonlinear lattices with on-site potential energy, such as the ϕ^4 and Frenkel–Kontorova (FK) lattices, exhibit normal heat conduction with length-independent heat conductivities.[15–17] Total momentum is conserved in 1D nonlinear lattices with interaction potential energy, but broken in those with on-site potential energy. It seems that momentum conservation plays a key role in determining the heat conduction behavior until normal heat conduction is found in the 1D coupled rotator lattice where total momentum is also conserved.[18–20] Unlike the well-known FPU-β lattice, the 1D coupled rotator lattice has a bounded interaction potential energy. Recently, the 1D coupled rotator lattice with additional bounded kinetic energy has been proposed, and normal heat conduction as well as energy diffusion behaviors have also been observed.[21,22] These studies demonstrate that bounded energy is essential for normal heat conduction in 1D momentum-conserving nonlinear lattices.

In determining the heat conduction behavior of 1D nonlinear lattices, a pseudo-saturation sometimes occurs due to finite-size effects when calculating the heat conductivity from non-equilibrium molecular dynamics as well as equilibrium Green–Kubo simulations.[23–27] In order to avoid pseudo-saturation, the equilibrium spatiotemporal correlation function method is applied to investigate energy diffusion.[28] The mean square displacement (MSD) of the energy $\langle \Delta x^2(t) \rangle_{\mathrm{E}}$ can be calculated to reveal the actual energy diffusion behavior. The power-law behavior of $\langle \Delta x^2(t) \rangle_{\mathrm{E}} \sim t^{\gamma}$ with $0 \le \gamma \le 2$ indicates normal energy diffusion when $\gamma = 1$ and anomalous superdiffusion when $\gamma > 1$.[28] It has been proved that heat conduction and energy diffusion can be directly related to each other as $\alpha = \gamma - 1$.[29] For normal energy diffusion, the corresponding spatiotemporal correlation function for local energy will exhibit a Gaussian distribution, where pseudo-saturation no longer occurs. Therefore, it is more convenient to investigate energy diffusion behavior in order to determine heat conduction behavior.[30–35]

In this work, we investigate the energy diffusion behavior of a 1D nonlinear momentum-conserving lattice with only bounded kinetic energy. Since stretch is another conserved quantity in this interacting lattice, its diffusion behavior will also be studied. Both the energy and stretch diffusion constants at different temperatures will be numerically resolved and discussed.

†Corresponding author. E-mail: nbli@hqu.edu.cn

‡Corresponding author. E-mail: jie@tongji.edu.cn

© 2025 Chinese Physical Society and IOP Publishing Ltd. All rights, including for text and data mining, AI training, and similar technologies, are reserved.

2. The Hamiltonian and numerical methods

The 1D momentum-conserving lattice with only bounded kinetic energy is described by the following Hamiltonian:

$$H=\sum_{i=1}^{N}H_i=\sum_{i=1}^{N}\left[(1-\cos p_i)+\frac{1}{2}(q_i-q_{i-1})^2\right], \tag{1}$$

where q_i, p_i, and H_i denote the displacement, momentum and local energy for the i-th atom. For simplicity and convenience, periodic boundary conditions are adopted with $q_0=q_N$ and $q_{N+1}=q_1$. The kinetic energy is bounded as a result of the trigonometric function $\cos p_i$. This lattice with periodic momentum serves as a toy model proposed for theoretical and numerical studies.

At the low-temperature limit $T\to 0$, the nonlinear kinetic energy can be expanded as

$$1-\cos p_i\approx 1-\left(1-\frac{1}{2}p_i^2\right)=\frac{1}{2}p_i^2, \tag{2}$$

and this lattice approaches the familiar 1D harmonic lattice.

For comparison, the 1D coupled rotator lattice has the Hamiltonian

$$H=\sum_{i=1}^{N}\left[\frac{1}{2}p_i^2+(1-\cos(q_i-q_{i-1}))\right], \tag{3}$$

and the 1D coupled rotator lattice with additional bounded kinetic energy has the Hamiltonian

$$H=\sum_{i=1}^{N}\left[(1-\cos p_i)+(1-\cos(q_i-q_{i-1}))\right]. \tag{4}$$

All three lattices share the property that at least one term of the energy, either kinetic or potential, is bounded, and their total momentum is conserved due to the interacting nature of their potential energy. It should be noted that the nonlinearity arises from the cosine term in each lattice.

For the current lattice with only bounded kinetic energy of Eq. (1), the probability distribution function ρ is

$$\rho=\frac{1}{Z}\mathrm{e}^{-\beta H}, \tag{5}$$

with $\beta=1/T$ denoting the inverse temperature, since the Boltzmann constant k_{B} is set to unity, and Z is the partition function given by

$$Z=\iint \mathrm{e}^{-\beta H}\,\mathrm{d}q_i\,\mathrm{d}p_i,\quad i=1,2,...,N. \tag{6}$$

The local temperature T_i can be expressed through the average local potential energy as

$$T_i=\left\langle (q_i-q_{i-1})^2\right\rangle, \tag{7}$$

where $\langle\cdot\rangle$ denotes the ensemble average, or equivalently the time average for chaotic systems. On the other hand, the local temperature can also be calculated by the following relation of local kinetic energy:[21,22]

$$\begin{aligned}1-\langle\cos p_i\rangle &= 1-\frac{\int_0^{2\pi}\cos p_i\,\mathrm{e}^{-\beta_i(1-\cos p_i)}\,\mathrm{d}p_i}{\int_0^{2\pi}\mathrm{e}^{-\beta_i(1-\cos p_i)}\,\mathrm{d}p_i}\\ &= 1-\frac{I_1(\beta_i)}{I_0(\beta_i)},\end{aligned} \tag{8}$$

with $I_0(x)$ and $I_1(x)$ the zeroth- and first-order modified Bessel functions of the first kind.

In Fig. 1, the energy density $e=\langle H_i\rangle$ and the average kinetic energy $1-\langle\cos p_i\rangle$ (both independent of the index i) are plotted as functions of the temperature T.

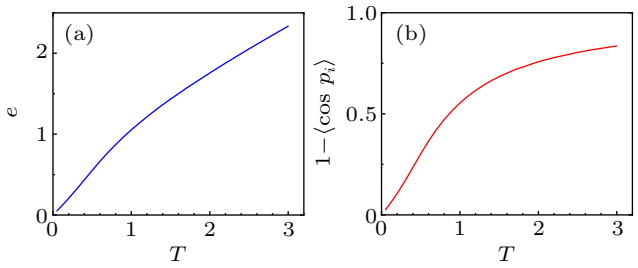


Fig. 1. (a) The energy density e as a function of temperature T. The energy density $e\approx T$ and $e\approx T/2$ in the low- and high-temperature limits, respectively. (b) The average kinetic energy $1-\langle\cos p_i\rangle$ as a function of temperature T.

Before we perform numerical simulations to study the energy diffusion of this lattice, the existence of thermal equilibrium should be verified. In Fig. 2, the equilibrium distributions of the kinetic energy $1-\langle\cos p_i\rangle$ have been plotted at three different temperatures with $T=0.2$, 0.4, and 0.7. The flat distributions of kinetic energy $1-\langle\cos p_i\rangle$ show that thermal equilibrium has been well established in this system at the designated temperatures.

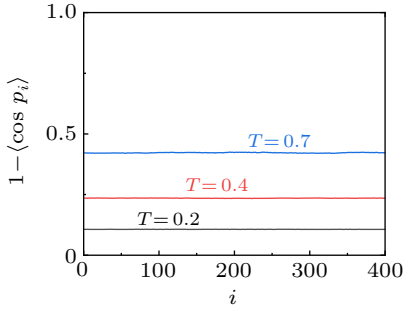


Fig. 2. Local distributions of kinetic energy $1-\langle\cos p_i\rangle$ at different temperatures T. Flat distributions indicate that thermal equilibrium has been established. The kinetic energy distributions are approximately 0.107, 0.235, and 0.422, corresponding to the input temperatures $T=0.2$ (bottom line, black), $T=0.4$ (middle line, red), and $T=0.7$ (top line, blue). The lattice size is $N=401$.

In order to investigate the energy and stretch diffusion behavior for this lattice, the equilibrium spatiotemporal correlation function method is applied.[28] The energy correlation function $C_{\mathrm{E}}(i,t)$ and the stretch correlation function $C_{\mathrm{S}}(i,t)$ are defined as[28]

$$C_{\mathrm{E}}(i,t)=\frac{\langle\Delta H_i(t)\Delta H_0(0)\rangle}{\langle\Delta H_0(0)\Delta H_0(0)\rangle}+\frac{1}{N-1}, \tag{9}$$

$$C_{\rm S}(i,t)=\frac{\langle\Delta(q_i(t)-q_{i-1}(t))\Delta(q_0(0)-q_{-1}(0))\rangle}{\langle\Delta(q_0(0)-q_{-1}(0))\Delta(q_0(0)-q_{-1}(0))\rangle}+\frac{1}{N-1},\tag{10}$$

where $\Delta A(t)=A(t)-\langle A(t)\rangle$ defines the real-time local fluctuation for energy $A=H_i$ and stretch $A=q_i-q_{i-1}$, respectively. For simplicity, the site index i is chosen from $-(N-1)/2$ to $(N-1)/2$, and an odd value of N is usually considered. The extra term $1/(N-1)$ arises from the use of a closed system with conserved total energy and stretch.[28] In the thermodynamic limit $N\to\infty$, this term will approach zero.

It is obvious that the correlation function $C_A(i,t=0)$ at the initial correlation time $t=0$ in the thermodynamic limit can be expressed as

$$C_{\rm E/S}(i,t=0)=\frac{\langle\Delta A_i(t=0)\Delta A_0(0)\rangle}{\langle\Delta A_0(0)\Delta A_0(0)\rangle}=\delta_{i,0},\tag{11}$$

which is a Kronecker delta function with $A=H$ or (q_i-q_{i-1}). These spatiotemporal correlation functions $C_{\rm E/S}(i,t)$ actually mimic the diffusion of energy and stretch fluctuations over the whole lattice. The information on energy and stretch diffusion is represented by the real-time spatiotemporal distributions of $C_{\rm E/S}(i,t)$.

The MSD $\langle\Delta x^2(t)\rangle_{\rm E/S}$ can be defined for energy and stretch as

$$\langle\Delta x^2(t)\rangle_{\rm E/S}=\sum_i i^2 C_{\rm E/S}(i,t).\tag{12}$$

The time dependence of MSD $\langle\Delta x^2(t)\rangle_{\rm E/S}$ is usually a power-law function, $\langle\Delta x^2(t)\rangle_{\rm E/S}\propto t^\gamma$, where $0\le\gamma\le 2$. In particular, an exponent of $\gamma=1$ corresponds to normal diffusion. The general relation $\alpha=\gamma-1$ between heat conduction and energy diffusion has been analytically proved,[29] enabling the investigation of heat conduction through the energy diffusion behavior via the equilibrium correlation function method.[28]

It is well known that normal diffusion behavior is characterized by the Gaussian distribution function

$$\rho_G(i,t)=\frac{1}{\sqrt{4\pi Dt}}\,{\rm e}^{-\frac{i^2}{4Dt}},\tag{13}$$

where D denotes the diffusion constant. If the correlation functions of energy or stretch $C_{\rm E/S}(i,t)$ approach the Gaussian distribution function after a transient correlation time, the corresponding diffusion process is normal. The appearance of a Gaussian distribution excludes the possible pseudo-saturation problem caused by size effects in other numerical methods such as the NEMD and equilibrium Green–Kubo method. As a result, the MSD $\langle\Delta x^2(t)\rangle_{\rm E/S}$ will show linear time dependence as

$$\langle\Delta x^2(t)\rangle_{\rm E/S}=\sum_i i^2\rho_G(i,t)=2D_{\rm E/S}t,\tag{14}$$

which is the property of the Gaussian distribution function.

In the numerical simulations, the fourth-order symplectic integration algorithm is applied with a time step $h=0.05$. The total simulation time is 5×10^7.

3. Results and discussion

In the low-temperature limit $T\to0$, where p_i is small, the Hamiltonian of the 1D momentum-conserving lattice with only bounded kinetic energy (Eq. (1)) approaches the 1D harmonic lattice. In this regime, the nonlinearity originating from the kinetic term is weak and the relaxation time for transport is long. Consequently, the transport coefficients, such as the energy and stretch diffusion constants, become very large due to the extended relaxation time.

In Fig. 3, the correlation functions of energy $C_{\rm E}(i,t)$ and stretch $C_{\rm S}(i,t)$ are plotted for a lattice of size $N=1201$ at a low temperature $T=0.2$. The results are shown at three different correlation times, $t=100$, 300, and 500. Although the functions exhibit different shapes, both $C_{\rm E}(i,t)$ and $C_{\rm S}(i,t)$ display a similar ballistic-like behavior, with wave fronts propagating symmetrically from the center toward the boundaries at a nearly constant sound speed $c_{\rm s}$. The observed sound speed $c_{\rm s}$ is slightly lower than unity, where $c_{\rm s}=1$ is the theoretical value for the 1D harmonic lattice.

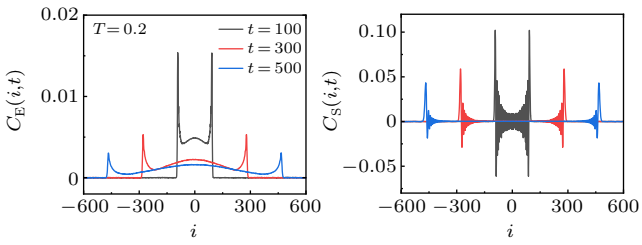


Fig. 3. The correlation function of energy $C_{\rm E}(i,t)$ (a) and stretch $C_{\rm S}(i,t)$ (b) for a lattice of size $N=1201$ at temperature $T=0.2$. The correlation functions at three different correlation times $t=100$, 300, and 500 are plotted as black, red, and blue solid lines (from center to two ends). At this low-temperature regime, both energy and stretch diffusions have very long relaxation times, with correlation lengths much larger than the lattice size $N=1201$ used here. Therefore, at $T=0.2$, only transient ballistic diffusion of energy and stretch can be observed due to finite-size effects. The sound speed $c_{\rm s}\approx1$, close to unity, which is the result for the harmonic lattice.

It should be noted that the energy and stretch diffusions at this low temperature are neither ballistic nor superdiffusive. This is because the correlation lengths of energy and stretch fluctuations are very large, exceeding the system size $N=1201$ used in the present simulations. The apparent "ballistic" behavior observed in Fig. 3 is merely a transient effect due to finite-size limitations, since the actual transport properties must be assessed in the thermodynamic limit $N\to\infty$. It is expected that normal diffusion of both energy and stretch would emerge in sufficiently larger systems, where correlation functions can be computed over longer correlation times. However, such simulations exceed our current computational

capability. Within the present numerical framework, no evidence of a transition from ballistic to normal diffusion is observed for this lattice model.

As temperature increases, the nonlinear effect due to the cosine function of momentum $\cos p_i$ begins to emerge. In Fig. 4(a), the correlation functions of energy $C_{\rm E}(i,t)$ at three different correlation times $t = 200$, 350, and 500 are plotted at higher temperature $T = 0.5$. It can be seen that at correlation time $t = 200$, the ballistic wave fronts have already disappeared and a bell shape curve like Gaussian distribution function of Eq. (13) shows up. At later correlation times of $t = 350$ and 500, the heights of the bell shape curves constantly decrease and their width broadens in the same time as a result of area conservation due to energy conservation.

In order to quantify the energy diffusion with the normal diffusion, the rescaled energy correlation functions $t^{1/2}C_{\rm E}(i,t)$ are plotted as the rescaled positions $i/t^{1/2}$ at correlation times $t = 200$, 350, and 500 in Fig. 4(b). It can be found that all three rescaled energy correlation functions $t^{1/2}C_{\rm E}(i,t)$ are almost overlapped with each other. The overlapped curve can be fitted with the Gaussian distribution function of Eq. (13). A fitting parameter $D_{\rm E} = 4.45$ is obtained. This Gaussian behavior confirms the normal energy diffusion behavior for this lattice and $D_{\rm E}$ can be explained as the diffusion constant for energy.

In Fig. 4(c), we plot the MSD $\langle \Delta x^2(t) \rangle_{\rm E}$ of energy as the function of correlation time t. The $\langle \Delta x^2(t) \rangle_{\rm E}$ shows an obvious linear correlation time dependence. A linear function of $\langle \Delta x^2(t) \rangle_{\rm E} = 2D_{\rm E}t$ with $D_{\rm E} = 4.45$ is plotted for comparison and the consistency with the numerical results can be viewed. Once the memory-free Gaussian distribution is obtained for the energy correlation function $C_{\rm E}(i,t)$, Gaussian behavior of the energy correlation function will be always observed for longer correlation time with larger lattice size.

At the same temperature $T = 0.5$, the stretch diffusion has also been investigated. In Fig. 5(a), we plot the correlation functions of stretch $C_{\rm S}(i,t)$ at three different correlation times $t = 200$, 350, and 500 for the same lattice size. It can be seen that for correlation time $t \geq 200$, the ballistic wave fronts previously observed at lower temperature $T = 0.2$ (seen in Fig. 3(b)) have disappeared and a similar bell shape curve like Gaussian distribution function of Eq. (13) shows up also.

In order to quantify the stretch diffusion with the possible normal diffusion, the rescaled stretch correlation functions $t^{1/2}C_{\rm S}(i,t)$ are plotted as the rescaled positions $i/t^{1/2}$ at correlation times $t = 200$, 350, and 500 in Fig. 5(b). Again the overlap for all these rescaled stretch $t^{1/2}C_{\rm S}(i,t)$ is observed. This overlapped function is fitted with the Gaussian distribution function of Eq. (13). A fitting parameter $D_{\rm S} = 3.80$ is numerically obtained. This Gaussian behavior also confirms the normal stretch diffusion behavior for this lattice and $D_{\rm S}$ can be explained as the diffusion constant for stretch. It should be noticed that the value of $D_{\rm S}$ is different from $D_{\rm E}$ at the same temperature.

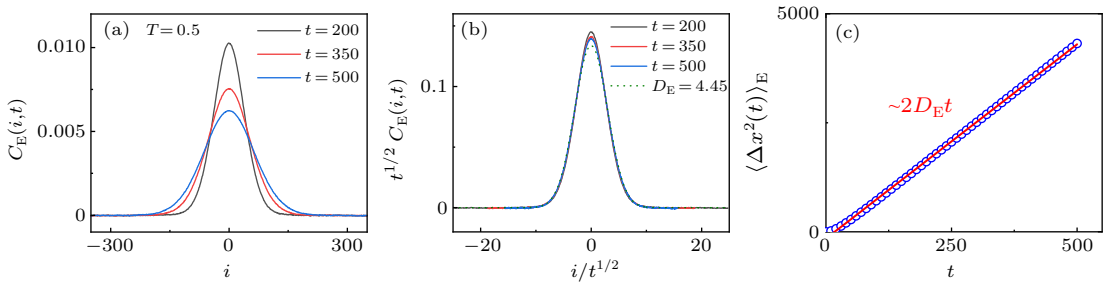


Fig. 4. The correlation function of energy $C_{\rm E}(i,t)$ for a lattice of size $N = 701$ at temperature $T = 0.5$. (a) The energy correlation functions $C_{\rm E}(i,t)$ are plotted at correlation times $t = 200$ (black), 350 (red), and 500 (blue), respectively. (b) The rescaled energy correlation function $t^{1/2}C_{\rm E}(i,t)$ as a function of the rescaled position $i/t^{1/2}$. The overlap of these three rescaled correlation functions $t^{1/2}C_{\rm E}(i,t)$ is clear, demonstrating Gaussian behavior. A Gaussian fitting of Eq. (13) yields an energy diffusion constant $D_{\rm E} = 4.45$. (c) The MSD $\langle \Delta x^2(t) \rangle_{\rm E}$ as a function of correlation time t. For comparison, the linear time behavior of $\langle \Delta x^2(t) \rangle_{\rm E} = 2D_{\rm E}t$ with $D_{\rm E} = 4.45$ is plotted, representing normal energy diffusion.

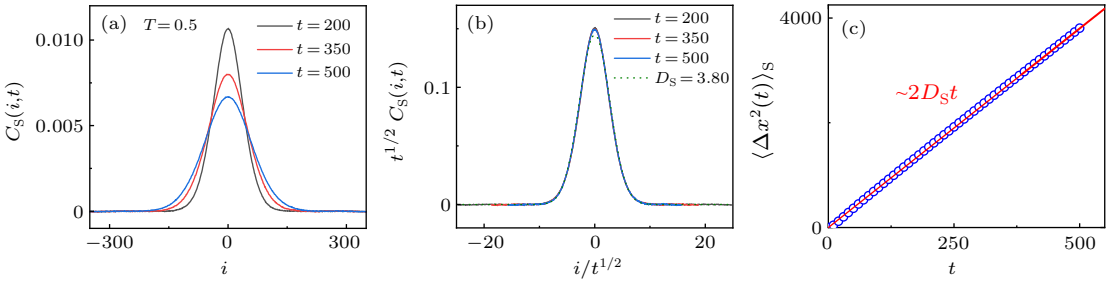


Fig. 5. The correlation function of stretch $C_{\rm S}(i,t)$ for a lattice of size $N = 701$ at temperature $T = 0.5$. (a) The stretch correlation functions $C_{\rm S}(i,t)$ are plotted at correlation times $t = 200$ (black), 350 (red), and 500 (blue), respectively. (b) The rescaled stretch correlation function $t^{1/2}C_{\rm S}(i,t)$ as a function of the rescaled position $i/t^{1/2}$. The overlap of these three rescaled correlation functions $t^{1/2}C_{\rm S}(i,t)$ demonstrates Gaussian behavior. A stretch diffusion constant $D_{\rm S} = 3.80$ is obtained from a Gaussian fit. (c) The MSD $\langle \Delta x^2(t) \rangle_{\rm S}$ as a function of correlation time t. The linear time dependence of $\langle \Delta x^2(t) \rangle_{\rm S} = 2D_{\rm S}t$ with $D_{\rm S} = 3.80$ is plotted, representing normal stretch diffusion.

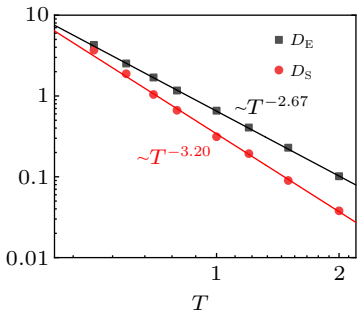


Fig. 6. The diffusion constants of energy D_E and stretch D_S as a function of temperature T. The black square symbols represent the numerical data for D_E, and the red circle symbols represent the numerical data for D_S. The energy diffusion constant D_E decreases with increasing temperature T, following a power-law behavior fitted as $D_E \propto T^{-2.67}$, while the stretch diffusion constant D_S decreases similarly, fitted as $D_S \propto T^{-3.20}$.

In Fig. 5(c), we plot the MSD $\langle \Delta x^2(t) \rangle_S$ of stretch as the function of correlation time t. The $\langle \Delta x^2(t) \rangle_S$ also shows an obvious linear correlation time dependence. A linear function of $\langle \Delta x^2(t) \rangle_S = 2D_S t$ with $D_S = 3.80$ is plotted for comparison and the consistency with the numerical results can be observed also. Therefore, the stretch diffusion in this lattice model possesses the same normal diffusion behavior as the energy diffusion but with a different value of diffusion constant.

At each temperature T, the diffusion constants of energy D_E and stretch D_S can be obtained by fitting the Gaussian distribution function or the linear time dependence of the corresponding MSD $\langle \Delta x^2(t) \rangle_{E/S}$. As a result, the temperature dependence of energy diffusion constant D_E and stretch diffusion constant D_S is plotted in Fig. 6. As can be seen from the figure, the energy diffusion constant D_E decreases as the temperature increases which can be fitted as a power-law behavior of $D_E \propto T^{-2.67}$. At the same time, the stretch diffusion constant D_S exhibits a similar power-law temperature dependence as $D_S \propto T^{-3.20}$. This temperature dependence is close to the temperature-dependent heat conductivity observed for 1D coupled rotator lattice where $\kappa \propto T^{-3.2}$.[36] In comparison to the 1D coupled rotator lattice where the displacement q_i is rotated, the current lattice has the rotated momentum p_i. In both lattices, the rotated term is bounded by a finite value as the temperature increases. Therefore, the temperature dependence of their transport coefficients exhibit similar power-law decreasing behaviors.

4. Conclusion

In conclusion, we have systematically investigated the energy and stretch diffusion behaviors for the 1D momentum-conserving lattice with a bounded kinetic energy term. The nonlinear part comes from the bounded kinetic energy containing the cosine function of the momentum $\cos p_i$ for every atom. The energy diffusion is found to exhibit normal diffusion similar to the previously studied momentum-conserving 1D coupled rotator lattice, where only potential energy is bounded, and the momentum-conserving 1D coupled rotator lattice with additional bounded kinetic energy, where both kinetic and potential energy are bounded. In addition, the stretch diffusion for the current lattice model also displays normal diffusion behavior. The temperature-dependent energy and stretch diffusion constants exhibit a power-law dependence of $D_{E/S} \propto T^{-\sigma}$ with σ around 3, which is similar to the temperature-dependent heat conductivity for the 1D coupled rotator lattice. Our work indicates that the bounded energy part, whether kinetic or potential, is essential to achieving normal energy diffusion or heat conduction.

Acknowledgments

Project supported by the National Natural Science Foundation of China (Grant Nos. 12175074 and 12475037) and the Science and Technology Commission of Shanghai Municipality (Grant No. 24520711200). J. C. is supported by the Shuguang Program of Shanghai Education Development Foundation and the Shanghai Municipal Education Commission (Grant No. 23SG18).

References

[1] Lepri S, Livi R and Politi A 1997 *Phys. Rev. Lett.* **78** 1896
[2] Lepri S, Livi R and Politi A 2003 *Phys. Rep.* **377** 1
[3] Dhar A 2008 *Adv. Phys.* **57** 457
[4] Liu S, Xu X F, Xie R G, Zhang G and Li B W 2013 *Eur. Phys. J. B* **85** 337
[5] Lepri S 2016 *Thermal Transport in Low Dimensions: From Statistical Physics to Nanoscale Heat Transfer* Vol. **921** (Heidelberg: Springer)
[6] Zhang Z W, Ouyang Y L, Cheng Y, Chen J, Li N B and Zhang G 2020 *Phys. Rep.* **860** 1
[7] Hatano T 1999 *Phys. Rev. E* **59** R1
[8] Prosen T and Campbell D K 2000 *Phys. Rev. Lett.* **84** 2857
[9] Narayan O and Ramaswamy S 2002 *Phys. Rev. Lett.* **89** 200601
[10] Pereverzev A 2003 *Phys. Rev. E* **68** 056124
[11] Wang J S and Li B W 2004 *Phys. Rev. Lett.* **92** 074302
[12] Wang L and Wang T 2011 *Europhys. Lett.* **93** 54002
[13] Wang L, Hu B and Li B W 2012 *Phys. Rev. E* **86** 040101
[14] Li N B, Li B W and Flach S 2010 *Phys. Rev. Lett.* **105** 054102
[15] Hu B, Li B W and Zhao H 1998 *Phys. Rev. E* **57** 2992
[16] Hu B, Li B W and Zhao H 2000 *Phys. Rev. E* **61** 3882
[17] Aoki K and Kusnezov D 2000 *Phys. Lett. A* **265** 250
[18] Giardinà C, Livi R, Politi A and Vassalli M 2000 *Phys. Rev. Lett.* **84** 2144
[19] Gendelman O and Savin A 2000 *Phys. Rev. Lett.* **84** 2381
[20] Li Y Y, Liu S, Li N B, Hänggi P and Li B W 2015 *New J. Phys.* **17** 043064
[21] Baldovin M and Iubini S 2021 *J. Stat. Mech.* 053202
[22] Chen H B and Li N B 2025 *Eur. Phys. J. B* **98** 21
[23] Zhong Y, Zhang Y, Wang J and Zhao H 2012 *Phys. Rev. E* **85** 060102(R)
[24] Savin A V and Kosevich Y A 2014 *Phys. Rev. E* **89** 032102
[25] Chen S, Zhang Y, Wang J and Zhao H 2016 *J. Stat. Mech.* 033205
[26] Wang L, Hu B and Li B W 2013 *Phys. Rev. E* **88** 052112
[27] Das S G, Dhar A and Narayan O 2014 *J. Stat. Phys.* **154** 204
[28] Zhao H 2006 *Phys. Rev. Lett.* **96** 140602
[29] Liu S, Hänggi P, Li N B, Ren J and Li B W 2014 *Phys. Rev. Lett.* **112** 040601
[30] Chen S, Zhang Y, Wang J. and Zhao H 2013 *Phys. Rev. E* **87** 032153
[31] Chen S, Zhang Y, Wang J and Zhao H 2014 *Phys. Rev. E* **89** 022111
[32] Wang L, Wu Z Y and Xu L 2015 *Phys. Rev. E* **91** 062130
[33] Xu L and Wang L 2017 *Phys. Rev. E* **96** 052139
[34] Li N B 2020 *J. Phys. D: Appl. Phys.* **53** 145302
[35] Li N B 2019 *Phys. Rev. E* **100** 062104
[36] Li Y Y, Li N B and Li B W 2015 *Eur. Phys. J. B* **88** 182